

**Nickel(II) Complexes of Schiff-base Ligands derived from the Condensation of 2,6-Diacetylpyridine with Ethanolamine ( $L^1$ ) or Propanolamine ( $L^2$ ); X-ray Crystal Structures of  $[\text{NiL}^1_2][\text{ClO}_4]_2 \cdot \text{H}_2\text{O}$ ,  $[\{\text{NiL}^1(\text{NCS})_2\}_2]$ ,  $[\text{NiL}^2_2][\text{ClO}_4]_2$ , and  $[\{\text{NiL}^2(\text{NCS})_2\}_x]$   $\{L^1 = 2,6\text{-bis}[1\text{-(2-hydroxyethylimino)ethyl}]\text{pyridine}$  and  $L^2 = 2,6\text{-bis}[1\text{-(3-hydroxypropylimino)ethyl}]\text{pyridine}\}^\dagger$**

Sally Brooker and Vickie McKee\*

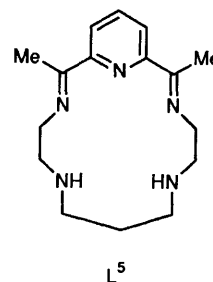
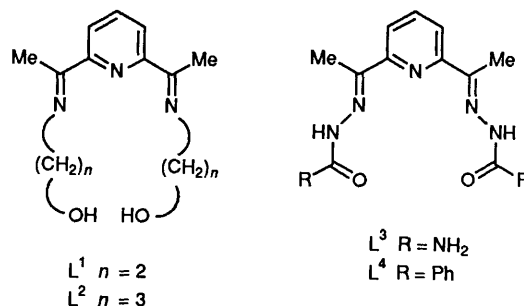
Department of Chemistry, University of Canterbury, Christchurch 1, New Zealand

Four structurally diverse nickel(II) complexes have been synthesised by Schiff-base condensation of 2,6-diacetylpyridine and ethanolamine  $\{L^1 = 2,6\text{-bis}[1\text{-(2-hydroxyethylimino)ethyl}]\text{pyridine}\}$  or propanolamine  $\{L^2 = 2,6\text{-bis}[1\text{-(3-hydroxypropylimino)ethyl}]\text{pyridine}\}$  in the presence of  $\text{Ni}^{2+}$ . These complexes have been characterised by combinations of analytical, spectroscopic, magnetic, conductance, and single-crystal X-ray diffraction methods:  $[\text{NiL}^1_2][\text{ClO}_4]_2 \cdot \text{H}_2\text{O}$  (1), monomeric, tetragonal,  $a = 10.109(1)$ ,  $c = 16.540(2)$  Å;  $[\{\text{NiL}^1(\text{NCS})_2\}_2]$  (2), dimeric, monoclinic,  $a = 12.623(4)$ ,  $b = 10.799(3)$ ,  $c = 14.174(5)$  Å,  $\beta = 106.61(3)^\circ$ ;  $[\text{NiL}^2_2][\text{ClO}_4]_2$  (3), monomeric, monoclinic,  $a = 19.482(4)$ ,  $b = 10.438(2)$ ,  $c = 21.324(5)$  Å,  $\beta = 123.48(2)^\circ$ ;  $[\{\text{NiL}^2(\text{NCS})_2\}_x]$  (4), polymeric, monoclinic,  $a = 14.922(7)$ ,  $b = 9.305(4)$ ,  $c = 16.140(7)$  Å, and  $\beta = 114.50(3)^\circ$ . Reasons for the structural diversity are discussed and comparisons are drawn with related complexes.

The open chain, Schiff-base ligand  $L^1$  provides five donor atoms; on co-ordination to manganese(II) these form a planar array which leads to the formation of pentagonal-bipyramidal manganese(II) complexes in which the pentagonal plane contains the three nitrogen and two alcohol donors of the ligand.<sup>1</sup> However lengthening the alkyl chains by one carbon atom ( $L^2$ ), results in pseudo-octahedral co-ordination of manganese(II). To complement our studies of these manganese complexes, the corresponding nickel complexes have been investigated and the results are presented in this paper. The most significant difference between the manganese(II) and nickel(II) ions lies in their electronic structures and consequent geometrical preferences. Manganese(II) is a  $d^5$  ion and will readily adopt the geometry imposed (even weakly) by a ligand, as is illustrated by the formation of seven co-ordinate complexes with  $L^1$ .<sup>1</sup> Nickel(II), in contrast, is a  $d^8$  ion and exhibits a marked preference for tetragonal geometries. It will form seven-co-ordinate complexes with conformationally rigid ligands such as  $L^3$  (ref. 2) and  $L^4$ .<sup>3</sup> However, the disfavoured nature of this geometry is illustrated by the behaviour of nickel(II) with the macrocyclic ligand  $L^5$ .<sup>4</sup> The only product isolated from this reaction contained the hydrolysed (at the imine) ring-opened ligand and the geometry of the complex was pseudo-octahedral. In contrast, manganese(II) forms stable seven-co-ordinate complexes with the same ligand.<sup>5</sup>

### Results and Discussion

**Synthesis.**—Condensation of 2,6-diacetylpyridine (dap) and ethanolamine on refluxing in benzene-methanol yielded the free ligand  $L^1$ . However, this product was contaminated by a carbonyl-containing material (probably unreacted dap) and was also somewhat unstable to hydrolysis. This freshly prepared free ligand can be used to prepare nickel complexes but, in general, better results were obtained when the condensation was carried out in the presence of nickel salts, yielding the complexes directly. This route was also used to prepare complexes of  $L^2$ . The thiocyanato complexes  $[\{\text{NiL}^1(\text{NCS})_2\}_2]$



(2) and  $[\{\text{NiL}^2(\text{NCS})_2\}_x]$  (4) were obtained as clean products from the reaction mixtures;  $[\text{NiL}^1_2][\text{ClO}_4]_2 \cdot \text{H}_2\text{O}$  (1) and  $[\text{NiL}^2_2][\text{ClO}_4]_2$  (3) are very soluble in all solvents tried and consequently were more difficult to obtain pure. Complexes (1) and (3) were obtained by evaporation of solvents almost to dryness and, consequently their yields and purity were somewhat variable.

<sup>†</sup> Supplementary data available: see Instructions for Authors, *J. Chem. Soc., Dalton Trans.*, 1990, Issue 1, pp. xix–xxii.

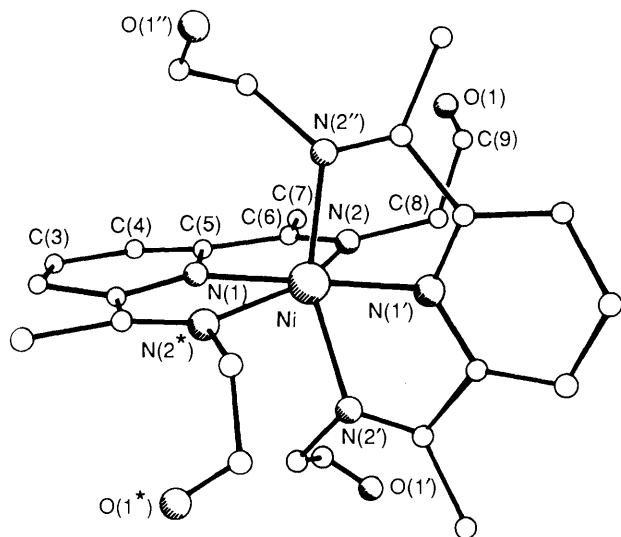


Figure 1. Perspective view of the cation  $[\text{NiL}^1_2]^{2+}$

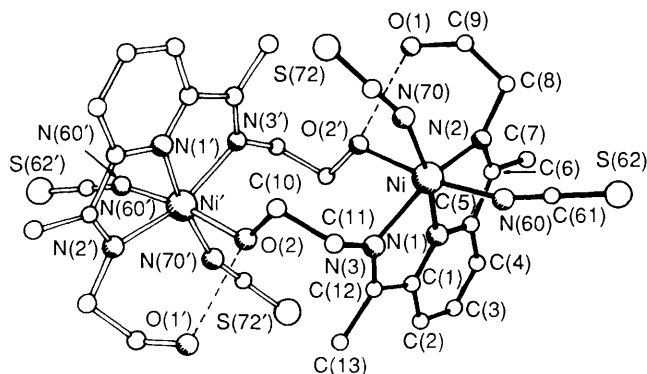


Figure 2. Perspective view of  $[\{\text{NiL}^1(\text{NCS})_2\}_2]^{2+}$ ; dotted lines represent hydrogen bonds

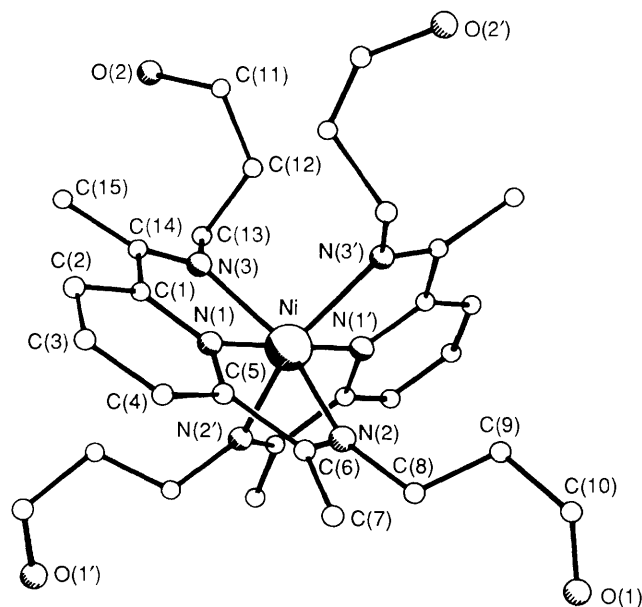


Figure 3. Perspective view of the cation  $[\text{NiL}^2_2]^{2+}$

**Physicochemical Studies.**—The i.r. spectra of each complex showed an absorption at *ca.* 1 650  $\text{cm}^{-1}$ , assigned to the  $\nu(\text{C}=\text{N})$

stretch of the imine bond. No  $\nu(\text{C}=\text{O})$  signal was observed, indicating that no unreacted dap remained in the samples. The perchlorate absorption of (1) is split with peaks at 1 150, 1 115, 1 085, and 1 040  $\text{cm}^{-1}$ . In the absence of hydrogen-bonding interactions (see below), the most likely reason is that crystal-packing effects disturb the site symmetry. The i.r. spectrum of complex (2) shows two sharp  $\nu(\text{O}-\text{H})$  absorptions (3 350 and 3 250  $\text{cm}^{-1}$ ). These arise from one co-ordinated alcohol group and from a hydrogen bond between this alcohol and the second, terminal alcohol group as seen in the X-ray structure. The X-ray structure determination revealed hydrogen bonding involving the alcohol groups in (3), however this is not obvious from the i.r. spectrum. No hydrogen bonding occurs in (4) but the bound alcohol group identified by the X-ray structure determination causes a sharp  $\nu(\text{O}-\text{H})$  absorption. The thiocyanate absorption of (4) is split (2 120 and 2 100  $\text{cm}^{-1}$ ); this can be ascribed to differences in the site symmetry of the two independent thiocyanate ligands.

Room-temperature magnetic moments have been measured for (2) and (4). Both complexes exhibit normal high-spin  $d^8$  behaviour<sup>6</sup> with moments of 3.0  $\mu_B$ .

Complexes (1) and (3) are red-brown whereas (2) and (4) are green. The electronic spectra are as expected for approximately octahedral nickel(II).<sup>4</sup> The lowest-energy band, *ca.* 805 nm for (1) and (3) and *ca.* 890 nm for (2) and (4), is assigned to the  ${}^3A_{2g} \rightarrow {}^3T_{2g}$  transition. The next absorption is a shoulder at *ca.* 505 nm for (1) and (3) whereas it is a well defined peak at *ca.* 585 nm for (2) and (4); this is assigned to the  ${}^3A_{2g} \rightarrow {}^3T_{1g}(F)$  transition. The third spin-allowed  $d-d$  transition is hidden by the much more intense charge-transfer and/or ligand transitions at higher energy. The difference between the two pairs of spectra can be attributed to the difference in donor sets. The six imine nitrogen donors present in (1) and (3) exert a considerably stronger ligand field than the mixed imine-thiocyanate-alcohol set of (2) and (4).

Conductivity measurements show that complexes (1) and (3) are 1:2 electrolytes in MeOH as expected. Some anion dissociation occurs on dissolution of (2) in dimethylformamide (dmf) and (4) in MeCN which behave as 1:1 and intermediate between a non-electrolyte and 1:1 electrolyte, respectively.

**Description of the Structures.**—The structures of this series of nickel(II) complexes  $[\text{NiL}^1_2][\text{ClO}_4]_2 \cdot \text{H}_2\text{O}$  (1),  $[\{\text{NiL}^1(\text{NCS})_2\}_2]$  (2),  $[\text{NiL}^2_2][\text{ClO}_4]_2$  (3) and  $[\{\text{NiL}^2(\text{NCS})_2\}_2]$  (4) are shown in Figures 1, 2, 3, and 4 [cations only for (1) and (3)]. Selected bond lengths and angles are given in Tables 1, 2, 3, and 4 respectively. In each of these structures the nickel(II) atom has a geometry approaching octahedral.

The two perchlorato complexes (1) and (3) are monomeric and have rather similar structures. In each case two ligand molecules are bound to the nickel atom *via* the nitrogen atoms only. The cation of complex (1) has crystallographically imposed  $\bar{4}$  symmetry, thus the angle between the mean planes of the two pyridine rings is constrained to 90°. The anisotropic thermal parameters associated with C(9) and O(1) are rather large; this is not unusual for a free saturated chain and is probably the result of some minor disorder in this region. The perchlorate anion has crystallographic  $C_2$  symmetry; the geometry of this group deviates considerably from tetrahedral but no attempt has been made to model this. Neither the perchlorate anion nor the lattice water molecule is involved in any hydrogen-bonding interactions.

In complex (3) the nickel atom is located on a  $C_2$  axis and the angle between the pyridine planes is 92.5°. The deviation from the expected value of 90° is small and is probably a result of packing effects associated with the saturated chains; in particular, the hydrogen bond between O(2) and an alcohol group [O(1')] of an adjacent cation is 2.73(1) Å. The

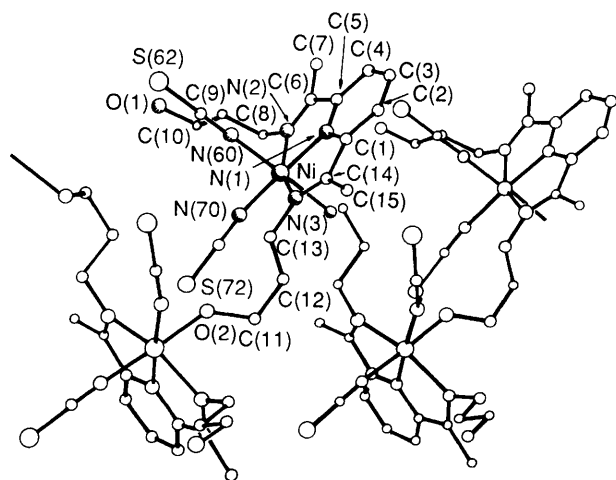


Figure 4. Perspective view of  $[\{\text{NiL}^2(\text{NCS})_2\}_x]$

Table 1. Selected interatomic distances (Å) and angles (°) for  $[\text{NiL}^1_2[\text{ClO}_4]_2]$  (1)

Ni-N(1)	1.981(13)	Ni-N(2)	2.117(12)
N(1)-Ni-N(2)	77.0(3)	N(1)-Ni-N(1')	180.0(1)
N(2)-Ni-N(1')	103.0(3)	N(2)-Ni-N(2')	92.9(1)
N(2)-Ni-N(2')	153.9(6)	N(2)-Ni-N(2'')	92.9(1)

Table 2. Selected interatomic distances (Å) and angles (°) for  $[\{\text{NiL}^1(\text{NCS})_2\}_2]$  (2)

Ni-N(1)	1.992(3)	Ni-N(2)	2.199(3)
Ni-N(3)	2.128(3)	Ni-N(70)	2.022(3)
Ni-N(60)	2.033(3)	Ni-O(2')	2.140(2)
N(1)-Ni-N(2)	76.6(1)	N(1)-Ni-N(3)	77.0(1)
N(2)-Ni-N(3)	153.5(1)	N(1)-Ni-N(70)	171.7(1)
N(2)-Ni-N(70)	109.1(1)	N(3)-Ni-N(70)	96.8(1)
N(1)-Ni-N(60)	94.4(1)	N(2)-Ni-N(60)	90.0(1)
N(3)-Ni-N(60)	94.4(1)	N(70)-Ni-N(60)	91.6(1)
N(1)-Ni-O(2')	91.0(1)	N(2)-Ni-O(2')	85.2(1)
N(3)-Ni-O(2')	92.9(1)	N(70)-Ni-O(2')	83.7(1)
N(60)-Ni-O(2')	171.7(1)	Ni-N(70)-C(71)	159.0(3)
Ni-N(60)-C(61)	161.9(3)		

perchlorate anion is in a general position and shows regular tetrahedral geometry with no significant intramolecular interactions.

A neutral dimer,  $[\{\text{NiL}^1(\text{NCS})_2\}_2]$  (2), is formed using  $\text{L}^1$  in the presence of strongly co-ordinating thiocyanate ions (Figure 2, Table 2). Each nickel atom is co-ordinated to the three nitrogen donors of one molecule of  $\text{L}^1$ ; the remaining co-ordination sites are filled by two nitrogen atoms of terminal thiocyanate groups and by one alcohol [O(2') or O(2)] group from the  $\text{L}^1$  ligand bound to the other nickel atom of the dimer. Thus, the dimer is held together by the intermolecular co-ordination of two alcohol groups. A hydrogen bond of 2.77(1) Å links O(1) and O(2') and the symmetry-related pair O(1') and O(2). The geometry about the nickel atom is closer to octahedral than in the two previous nickel complexes because only one pyridinedi-imine is bound per nickel atom. The two less geometrically constrained thiocyanate groups and the alcohol ligands make angles with each other about the nickel atom which approach 90° (Table 2).

A polymeric nickel(II) complex  $[\{\text{NiL}^2(\text{NCS})_2\}_x]$  (4) is

Table 3. Selected interatomic distances (Å) and angles (°) for  $[\text{NiL}^2_2[\text{ClO}_4]_2]$  (3)

Ni-N(1)	1.973(3)	Ni-N(2)	2.106(2)
Ni-N(3)	2.125(2)		
N(1)-Ni-N(2)	78.1(1)	N(1)-Ni-N(3)	77.1(1)
N(2)-Ni-N(3)	154.7(1)	N(1)-Ni-N(1')	178.9(1)
N(2)-Ni-N(1')	102.7(1)	N(3)-Ni-N(1')	102.2(1)
N(3)-Ni-N(3')	99.8(1)	N(2)-Ni-N(2')	90.7(1)
N(3)-Ni-N(2')	90.1(1)		

Table 4. Selected interatomic distances (Å) and angles (°) for  $[\{\text{NiL}^2(\text{NCS})_2\}_x]$  (4)

Ni-N(1)	1.993(4)	Ni-N(2)	2.109(6)
Ni-N(3)	2.123(6)	Ni-N(60)	2.066(5)
Ni-N(70)	2.016(4)	Ni-O(2')	2.177(4)
N(1)-Ni-N(2)	77.3(2)	N(1)-Ni-N(3)	77.6(2)
N(2)-Ni-N(3)	154.9(2)	N(1)-Ni-N(60)	93.1(2)
N(2)-Ni-N(60)	91.2(2)	N(3)-Ni-N(60)	90.6(2)
N(1)-Ni-N(70)	175.4(2)	N(2)-Ni-N(70)	102.1(2)
N(3)-Ni-N(70)	102.9(2)	N(60)-Ni-N(70)	91.5(2)
N(1)-Ni-O(2')	88.1(2)	N(2)-Ni-O(2')	91.0(2)
N(3)-Ni-O(2')	87.7(2)	N(60)-Ni-O(2')	177.7(2)
N(70)-Ni-O(2')	87.3(2)	Ni-N(60)-C(61)	173.7(5)
Ni-N(70)-C(71)	161.8(6)		

isolated with  $\text{L}^2$  and thiocyanate (Figure 4, Table 4). Each nickel atom binds one  $\text{L}^2$  ligand via the three nitrogen donors; two nitrogen atoms of terminally bound thiocyanate groups and the terminal alcohol oxygen of a flexible alkyl chain from a different unit complete the co-ordination sphere. As with the dimer (2), the link between successive units in the polymer is the intermolecular co-ordination of an alcohol chain. Again, as observed for (2), the unconstrained thiocyanate and alcohol donors adopt geometries close to octahedral and deviations from regular geometry are due to the  $\text{L}^2$  ligand. The mean planes of successive pyridine rings in the chain make angles of 63.7° with each other.

Within this series, distortions from regular octahedral geometry are due to the binding of one or two pyridinedi-imine units, each of which enforces bonding of three donors within an arc of approximately 150°. In each of the complexes the Ni-N(pyridine) bond is significantly shorter than the Ni-N(imine) distances. This is a result of three factors: the relative rigidity of the pyridinedi-imine unit, the radius of the metal ion, and the preference of nickel for octahedral geometry. Since the three nitrogen donors are fixed with respect to one another, the N(pyridine)-metal-N(imine) angle depends on the M-N(pyridine) distance; this in turn is largely controlled by the radius of the metal ion. The nickel(II) complexes (metal-ion radius 0.83 Å, ref. 7) have N(pyridine)-Ni-N(imine) angles in the range 76.6(1)–78.1(1)°, whereas with the large manganese(II) ion (radius 0.93 Å, ref. 7) this angle is reduced to 68.2(1)–71.2(1)°. The metal-N(imine) distance is then fixed by the ligand geometry.

## Conclusion

These four nickel(II) complexes form an interesting structural series with nuclearities ranging from monomeric through dimeric to polymeric. However, despite this diversity all of these complexes are six-co-ordinate. This is in contrast to the seven-

co-ordinate nickel(II) complexes of the planar resonance-stabilised ligands  $L^3$  (ref. 2) and  $L^4$  (ref. 3) and the seven-co-ordinate manganese(II) complexes of  $L^1$  (ref. 1). Ligand  $L^1$  can provide a pentagonal plane of donor atoms as seen in the series of manganese(II) complexes but when it binds nickel(II) the alcohol groups twist away from the central nickel atom and only the  $N_3$  donor set bonds. This demonstrates that seven-co-ordination is not enforced by  $L^1$ , and when nickel(II) is bound the preference for tetragonal geometries dominates. A very similar result was observed by Nelson and co-workers<sup>4</sup> when attempts were made to complex nickel(II) with the macrocyclic ligand  $L^5$ . The preference of the  $d^8$  nickel(II) ion for tetragonal geometry led to hydrolysis of an imine bond to release strain, resulting in a six-co-ordinate complex of the ring-opened ligand.

As seen in the manganese complexes of  $L^1$  and  $L^2$  (ref. 1), no alkoxy bridging of two metal ions is observed in these nickel complexes. However, intermolecular alcohol binding does lead to the formation of dimeric (2) and polymeric (4) complexes.

### Experimental

**Preparation of Complexes.**— $[NiL^1_2][ClO_4]_2 \cdot H_2O$  (1). 2,6-Diacetylpyridine (dap) (1 g, 6.1 mmol) and excess of ethanolamine (1.75 g, 28.7 mmol) were refluxed in a benzene-dry methanol mixture, removing the azeotrope, for many hours. Most of the excess of ethanolamine separated from the final benzene solution allowing it to be removed. This preparation of  $L^1$  [i.r. spectrum showed only a small  $\nu(C=O)$ ] was used immediately in the following reaction. The salt  $Ni(ClO_4)_2 \cdot 6H_2O$  (0.75 g, 2.1 mmol) in dry methanol (15 cm<sup>3</sup>) was added to free  $L^1$  (2.1 mmol) in benzene (15 cm<sup>3</sup>). The resulting clear yellow-brown solution was stoppered and allowed to stand for 2 d. After evaporating the solution to 10 cm<sup>3</sup> under reduced pressure,  $Pr^iOH$  was added until the solution became cloudy. Benzene and methanol were then added until the solution cleared again. Slow evaporation over 2 months yielded red-brown crystals suitable for a single-crystal X-ray structure determination, in a brown oil. I.r. data: 3 370s(br), 1 635w, 1 585m, 1 150s, 1 115s, 1 085s, and 1 040s cm<sup>-1</sup>.  $\Lambda_m(MeOH) = 182 \text{ ohm}^{-1} \text{ cm}^2 \text{ mol}^{-1}$  (lit.,<sup>8</sup> 1:2 160–220 ohm<sup>-1</sup> cm<sup>2</sup> mol<sup>-1</sup>). Electronic spectrum (MeOH):  $\lambda_{max.} = 804$  ( $\epsilon = 40 \text{ dm}^3 \text{ mol}^{-1} \text{ cm}^{-1}$ ) and 510 (sh) nm. Fast atom bombardment mass spectrum:  $m/z$  655,  $[NiL^1_2(ClO_4)]^+$ .

$[NiL^1(NCS)_2]_2$  (2). The salt  $Ni(ClO_4)_2 \cdot 6H_2O$  (2.46 g, 6.7 mmol) in methanol (10 cm<sup>3</sup>) was added to a refluxing methanolic solution (50 cm<sup>3</sup>) of dap (1 g, 6.1 mmol). This was followed by the dropwise addition of ethanolamine (0.75 g, 6.1 mmol) in methanol (5 cm<sup>3</sup>), and finally the addition of NaNCS (1.10 g, 13.6 mmol) in methanol (15 cm<sup>3</sup>). The resulting mid-green solution was refluxed for 3 h over which time the solution became darker green. The solution was allowed to cool slowly and the green crystalline solid which precipitated was collected by filtration. Further crops were obtained after slow evaporation of the solvent. Yield 0.76 g, 1.8 mmol, 30%. Recrystallisation by vapour diffusion of diethyl ether, from  $dmf-EtOH$ , in the presence of excess of NaNCS produced green plates suitable for a single-crystal X-ray structure determination (Found: C, 42.6; H, 4.6; N, 16.2. Calc. for  $C_{30}H_{38}N_{10}Ni_2O_4S_4$ : C, 42.5; H, 4.5; N, 16.5%). I.r. data: 3 350m, 3 250m, 2 090s, 1 640m, and 1 595m cm<sup>-1</sup>. Magnetic moment (298 K) = 3.0  $\mu_B$ .  $\Lambda_m(dmf) = 108 \text{ ohm}^{-1} \text{ cm}^2 \text{ mol}^{-1}$  (lit.,<sup>8</sup> 1:1, 65–90 ohm<sup>-1</sup> cm<sup>2</sup> mol<sup>-1</sup>). Electronic spectrum: (solid),  $\lambda_{max.} = 960, 590$ ; (dmf),  $\approx 890$  ( $\epsilon = 70$ ) and 585 nm (40 dm<sup>3</sup> mol<sup>-1</sup> cm<sup>-1</sup>).

$[NiL^2_2][ClO_4]_2$  (3). Propanolamine (0.92 g, 12.3 mmol) in ethanol (5 cm<sup>3</sup>) was added dropwise to a refluxing ethanol (50 cm<sup>3</sup>) solution of dap (1 g, 6.1 mmol) and  $Ni(ClO_4)_2 \cdot 6H_2O$  (1.12 g, 3.1 mmol) causing the colour to change from green to dark

red-brown. Most of the resulting precipitate redissolved during the following 3-h reflux; that remaining was removed by filtration. Slow evaporation of the solvent allowed the formation of red-brown crystals suitable for single-crystal analysis. Recrystallisation by vapour diffusion of diethyl ether into a MeCN solution also led to the formation of good crystals. Yield 26% [Found: C, 44.9; H, 5.8; N, 10.6. Calc. for (3)·0.5 MeCN: C, 44.7; H, 5.7; N, 10.9%]. I.r. data: 3 330s(br), 1 625m, 1 590m, and 1 100s(br) cm<sup>-1</sup>.  $\Lambda_m(MeOH) = 152 \text{ ohm}^{-1} \text{ cm}^2 \text{ mol}^{-1}$  (lit.,<sup>8</sup> 1:2, 160–220 ohm<sup>-1</sup> cm<sup>2</sup> mol<sup>-1</sup>). Electronic spectrum (MeOH):  $\lambda_{max.} = 806$  ( $\epsilon = 40 \text{ dm}^3 \text{ mol}^{-1} \text{ cm}^{-1}$ ) and 505 (sh) nm.

$[NiL^2(NCS)_2]_2$  (4). The salt  $Ni(ClO_4)_2 \cdot 6H_2O$  (2.24 g, 6.1 mmol) in methanol (10 cm<sup>3</sup>) was added to a refluxing methanol (50 cm<sup>3</sup>) solution of dap (1 g, 6.1 mmol). Dropwise addition of propanolamine (0.92 g, 12.2 mmol) in methanol (5 cm<sup>3</sup>) caused the yellow-green solution to turn dark brown. Sodium thiocyanate (1.00 g, 12.2 mmol) in methanol (15 cm<sup>3</sup>) was quickly added and the dark brown solution refluxed for 40 min. Four days later, green crystals suitable for X-ray analysis were filtered from the brown solution. A dichroic brown/green crystal was shown to be the same compound by an X-ray unit-cell determination. After slow evaporation of solvent further crops of green crystalline product were obtained. Yield 1.83 g, 4.1 mmol, 66% calculated on monomer molecular weight (Found: C, 45.1; H, 5.1; N, 15.1. Calc. for  $C_{17}H_{23}N_5NiO_2S_2$ : C, 45.1; H, 5.1; N, 15.5%). I.r. data: 3 400m(br), 3 310m, 2 120s, 2 100s, 1 635w, and 1 595m cm<sup>-1</sup>. Magnetic moment (298 K) = 3.0  $\mu_B$ .  $\Lambda_m(MeCN) = 45 \text{ ohm}^{-1} \text{ cm}^2 \text{ mol}^{-1}$  (lit.,<sup>8</sup> 1:1, 120–160 ohm<sup>-1</sup> cm<sup>2</sup> mol<sup>-1</sup>). Electronic spectrum (solid),  $\lambda_{max.} = 920, 580$ ; (dmf),  $\approx 892$  ( $\epsilon = 30$ ) and 585 nm (15 dm<sup>3</sup> mol<sup>-1</sup> cm<sup>-1</sup>).

**Crystallography.**—X-Ray crystallographic data were collected on a Nicolet R3m four-circle diffractometer using graphite-monochromated Mo- $K_\alpha$  radiation ( $\lambda = 0.71069 \text{ \AA}$ ). The diffractometer was equipped with a locally modified Nicolet LT-1 low-temperature attachment. The unit-cell parameters were determined by least squares refinement of 17–25 accurately centred reflections in the range  $5 < 2\theta < 35^\circ$ . Crystal stability was monitored by recording three check reflections every 97 reflections and no significant variations were observed for any data sets. The data were corrected for Lorentz and polarisation effects and empirical absorption corrections were applied, based on  $\psi$ -scan data. There was no evidence of extinction in any of the data sets. Hydrogen atoms were inserted at calculated positions using a riding model with thermal parameters equal to 1.2U of their carrier atoms. The function minimised in the refinement was  $\sum w(|F_o| - |F_c|)^2$  where  $w = [\sigma^2(F_o) + gF_o^2]^{-1}$ . Final atom co-ordinates are given in Table 5. All programs used in data reduction and final refinement were contained in the SHELXTL (version 4.0) package;<sup>9</sup> SHELXTL or SHELXS<sup>10</sup> was employed to solve the structures, and in some cases the intermediate refinement was performed using SHELX 76.<sup>11</sup>

Additional material available from the Cambridge Crystallographic Data Centre comprises H-atom co-ordinates, thermal parameters, and remaining bond lengths and angles.

**Crystal data.** For  $[NiL^1_2][ClO_4]_2 \cdot H_2O$  (1).  $C_{26}H_{40}Cl_2NiN_6O_{13}$ , irregular brown block, crystal dimensions 0.25 × 0.47 × 0.47 mm, tetragonal, space group  $P4_2/c$ ,  $a = 10.109(1)$ ,  $c = 16.540(2) \text{ \AA}$ ,  $U = 1690.2(5) \text{ \AA}^3$ ,  $Z = 2$ ,  $F(000) = 808$ ,  $\mu = 0.80 \text{ mm}^{-1}$ .

Using  $1.4^\circ \omega$  scans at a scan rate of  $3.91^\circ \text{ min}^{-1}$ , 1 723 reflections were collected with  $4 < 2\theta < 50^\circ$  at room temperature. Of these, 857 were unique, and the 554 having  $I > 3\sigma(I)$  were ultimately used in the structure refinement. A Patterson calculation<sup>9</sup> revealed the position of the nickel atom and the remaining non-hydrogen atoms were located from Fourier difference maps. Hydrogen atoms were inserted on all but the quarter-occupancy water molecule O(20). Anisotropic thermal parameters were

Table 5. Atomic co-ordinates ( $\times 10^4$ )

Atom	x	y	z	Atom	x	y	z
<b>[NiL<sup>1</sup><sub>2</sub>][ClO<sub>4</sub>]<sub>2</sub> (1)</b>							
Ni	0	0	5 000	C(8)	-2 148(21)	-2 194(22)	5 360(11)
N(1)	0	0	3 802(8)	C(9)	-1 662(42)	-3 404(32)	5 534(15)
C(3)	0	0	2 176(10)	O(1)	-1 907(25)	-4 149(36)	5 173(14)
C(4)	-968(20)	-775(17)	2 575(8)	Cl	-5 000	0	2 050(4)
C(5)	-842(16)	-823(15)	3 420(8)	O(11)	-5 561(19)	892(22)	1 578(11)
C(6)	-1 716(11)	-1 546(17)	3 977(11)	O(12)	-5 854(21)	-623(21)	2 680(8)
C(7)	-2 820(19)	-2 371(18)	3 569(11)	O(20)	0	0	0
N(2)	-1 491(13)	-1 393(11)	4 711(6)				
<b>[{NiL<sup>1</sup>(NCS)<sub>2</sub>]<sub>2</sub> (2)</b>							
Ni	4 436(1)	6 814(1)	6 259(1)	C(10)	6 542(3)	4 690(3)	5 740(2)
N(1)	4 027(2)	8 010(2)	5 144(2)	O(2)	6 341(2)	4 667(2)	4 691(2)
C(1)	4 755(3)	8 259(3)	4 644(2)	C(11)	6 796(3)	6 002(3)	6 134(2)
C(2)	4 510(3)	9 120(3)	3 883(2)	N(3)	5 848(2)	6 800(3)	5 723(2)
C(3)	3 507(3)	9 725(3)	3 659(3)	C(12)	5 804(3)	7 531(3)	4 995(2)
C(4)	2 760(3)	9 448(3)	4 172(3)	C(13)	6 668(3)	7 699(3)	4 469(3)
C(5)	3 035(3)	8 578(3)	4 918(2)	N(70)	4 938(2)	5 444(3)	7 260(2)
C(6)	2 324(3)	8 181(3)	5 542(3)	C(71)	5 265(3)	4 487(3)	7 579(2)
C(7)	1 204(3)	8 757(4)	5 328(3)	S(72)	5 744(1)	3 135(1)	8 033(1)
N(2)	2 744(2)	7 367(3)	6 208(2)	N(60)	5 050(2)	8 133(3)	7 294(2)
C(8)	2 102(3)	6 940(4)	6 865(3)	C(61)	5 233(3)	8 709(3)	8 007(2)
C(9)	2 361(3)	5 607(4)	7 167(3)	S(62)	5 493(1)	9 547(1)	9 011(1)
O(1)	2 157(2)	4 791(2)	6 344(2)				
<b>[NiL<sup>2</sup><sub>2</sub>][ClO<sub>4</sub>]<sub>2</sub> (3)</b>							
Ni	5 000	7 821(1)	7 500	O(1)	6 802(1)	11 464(2)	10 182(1)
N(1)	5 710(1)	7 804(2)	7 107(1)	O(2)	3 444(1)	3 253(2)	5 855(1)
C(1)	5 505(2)	7 060(3)	6 518(2)	C(11)	3 970(2)	3 619(3)	6 628(2)
C(2)	5 990(2)	7 056(3)	6 223(2)	C(12)	3 655(2)	4 805(3)	6 799(2)
C(3)	6 679(2)	7 840(3)	6 560(2)	C(13)	3 577(2)	5 969(3)	6 339(2)
C(4)	6 877(2)	8 603(3)	7 166(2)	N(3)	4 387(1)	6 510(2)	6 588(1)
C(5)	6 367(2)	8 572(3)	7 430(2)	C(14)	4 723(2)	6 342(3)	6 219(2)
C(6)	6 451(2)	9 382(3)	8 049(2)	C(15)	4 398(2)	5 560(3)	5 517(2)
C(7)	7 167(2)	10 273(3)	8 447(2)	Cl	3 953(1)	12 504(1)	8 683(1)
N(2)	5 875(1)	9 240(2)	8 162(1)	O(11)	3 871(2)	13 812(3)	8 463(2)
C(8)	5 837(2)	10 045(3)	8 709(2)	O(12)	4 685(3)	12 332(4)	9 398(2)
C(9)	6 298(2)	9 445(3)	9 493(2)	O(13)	3 967(3)	11 742(4)	8 155(2)
C(10)	6 316(2)	10 346(3)	10 061(2)	O(14)	3 278(3)	12 222(4)	8 724(3)
<b>[{NiL<sup>2</sup>(NCS)<sub>2</sub>]<sub>2</sub> (4)</b>							
Ni	8 002(1)	333(1)	2 079(1)	O(2)	11 156(3)	3 360(4)	2 754(2)
N(1)	7 007(3)	-469(5)	916(3)	C(11)	11 246(4)	2 160(7)	2 219(4)
C(1)	7 145(4)	-277(6)	152(4)	C(12)	10 363(4)	1 153(7)	1 921(4)
C(2)	6 469(4)	-827(6)	-671(4)	C(13)	9 413(4)	1 959(7)	1 374(4)
C(3)	5 670(4)	-1 591(7)	-659(4)	N(3)	8 551(3)	1 001(5)	1 119(3)
C(4)	5 534(4)	-1 781(7)	134(4)	C(14)	8 055(4)	581(6)	304(4)
C(5)	6 234(4)	-1 187(6)	928(4)	C(15)	8 281(4)	848(7)	-513(4)
C(6)	6 238(4)	-1 238(6)	1 856(4)	N(60)	7 252(3)	2 252(3)	1 922(3)
C(7)	5 366(4)	-1 868(7)	1 968(4)	C(61)	6 834(4)	3 320(7)	1 915(4)
N(2)	7 006(3)	-715(5)	2 498(3)	S(62)	6 225(1)	4 793(2)	1 869(1)
C(8)	7 118(4)	-725(6)	3 446(4)	N(70)	9 061(3)	988(5)	3 275(3)
C(9)	6 719(5)	625(7)	3 686(4)	C(71)	9 777(4)	1 493(7)	3 808(4)
C(10)	6 958(5)	694(7)	4 698(4)	S(72)	10 781(1)	2 259(2)	4 535(1)
O(1)	6 609(3)	2 009(5)	4 876(3)				

assigned to all non-hydrogen atoms and the refinement on 110 parameters converged with  $R = 0.0896$ ,  $R' = 0.1238$ ,  $g = 0.000633$ , and a maximum least-squares shift/error of 0.024. The final difference map showed no features greater than  $\pm 0.87$  e  $\text{\AA}^{-3}$ .

For  $[{\text{NiL}}^1(\text{NCS})_2]_2$  (2).  $\text{C}_{30}\text{H}_{38}\text{N}_{10}\text{Ni}_2\text{O}_4\text{S}_4$ , green plate, crystal dimensions  $0.06 \times 0.30 \times 0.46$  mm, monoclinic, space group  $P2_1/n$ ,  $a = 12.623(4)$ ,  $b = 10.799(3)$ ,  $c = 14.174(5)$   $\text{\AA}$ ,  $\beta = 106.61(3)^\circ$ ,  $U = 1 851(1)$   $\text{\AA}^3$ ,  $Z = 2$ ,  $F(000) = 880$ ,  $\mu = 1.29$   $\text{mm}^{-1}$ .

Using  $1.6^\circ$   $\omega$  scans at a scan rate of  $4.88^\circ \text{min}^{-1}$ , 3 588 reflections were collected with  $4 < 2\theta < 50^\circ$  at 173 K. Of these, 3 248 were unique, and the 2 414 having  $I > 3\sigma(I)$  were ultimately used in the structure refinement. A Patterson calculation<sup>9</sup> revealed the position of the nickel atom and the remaining non-hydrogen atoms were located from Fourier difference maps. Anisotropic thermal parameters were assigned to all non-hydrogen atoms and refinement on 226 parameters converged with  $R = 0.0343$ ,  $R' = 0.0445$ ,  $g = 0.000 67$ , and a maximum least-squares shift/error of 0.011.

The final difference map showed no features greater than  $\pm 0.6 \text{ e } \text{Å}^{-3}$ .

For  $[\text{NiL}^2_2][\text{ClO}_4]_2$  (3).  $\text{C}_{30}\text{H}_{46}\text{Cl}_2\text{N}_6\text{NiO}_{12}$ , irregular red-brown block, crystal dimensions  $0.20 \times 0.30 \times 0.49 \text{ mm}$ , monoclinic, space group  $C2/c$ ,  $a = 19.482(4)$ ,  $b = 10.438(2)$ ,  $c = 21.324(5) \text{ Å}$ ,  $\beta = 123.48(2)^\circ$ ,  $U = 3\ 616(2) \text{ Å}^3$ ,  $Z = 4$ ,  $F(000) = 1\ 704$ ,  $\mu = 0.75 \text{ mm}^{-1}$ .

Using  $1.4^\circ \omega$  scans at a scan rate of  $4.88^\circ \text{ min}^{-1}$ , 3 469 reflections were collected with  $4 < 2\theta < 50^\circ$  at 153 K. Of these, 3 186 were unique, and the 2 572 having  $I > 3\sigma(I)$  were ultimately used in the structure refinement. A Patterson calculation<sup>9</sup> revealed the position of the nickel atom and the remaining non-hydrogen atoms were located from Fourier difference maps. Anisotropic thermal parameters were assigned to all non-hydrogen atoms and refinement on 231 least-squares parameters converged with  $R = 0.0409$ ,  $R' = 0.0555$ ,  $g = 0.00067$ , and a maximum least-squares shift/error of 0.02. The final difference map showed no features greater than  $\pm 0.6 \text{ e } \text{Å}^{-3}$ .

For  $[\{\text{NiL}^2(\text{NCS})_2\}_x]$  (4).  $\text{C}_{17}\text{H}_{23}\text{N}_5\text{NiO}_2\text{S}_2$ , green plate, crystal dimensions  $0.13 \times 0.22 \times 0.59 \text{ mm}$ , monoclinic, space group  $P2_1/c$ ,  $a = 14.922(7)$ ,  $b = 9.305(4)$ ,  $c = 16.140(7) \text{ Å}$ ,  $\beta = 114.50(3)^\circ$ ,  $U = 2\ 039(1) \text{ Å}^3$ ,  $Z = 4$ ,  $F(000) = 944$ ,  $\mu = 1.17 \text{ mm}^{-1}$ .

Using  $1.9^\circ \omega$  scans at a scan rate of  $4.19^\circ \text{ min}^{-1}$ , 4 338 reflections were collected with  $4 < 2\theta < 50^\circ$  at 140 K. Of these, 3 792 were unique, and the 2 049 having  $I > 3\sigma(I)$  were ultimately used in the structure refinement. Direct methods<sup>10</sup> revealed the structure and the remaining non-hydrogen atoms were located from Fourier difference maps. Anisotropic thermal parameters were assigned to all non-hydrogen atoms and refinement on 245 least-squares parameters converged with  $R = 0.0490$ ,  $R' = 0.0456$ ,  $g = 0.000\ 18$ , and a maximum least-squares shift/error of 0.03. The final difference map showed no features greater than  $\pm 0.56 \text{ e } \text{Å}^{-3}$ .

Infrared spectra were recorded as KBr discs using a Pye-Unicam SP3-300 spectrometer. A Varian DMS100 spectro-

photometer was used to record electronic spectra of solutions over the range 200–900 nm. Spectra of solid samples were recorded using a Beckman DK-2A ratio recording spectrophotometer. Room-temperature magnetic moment measurements were carried out using a Newport Instruments Gouy balance. Microanalyses were by the Campbell Microanalytical Laboratory, University of Otago, Dunedin. A Wayne Kerr Universal Bridge B224 in conjunction with a conductivity cell (platinum electrodes) of cell constant 0.251 was used for measurements of electrical conductance.

### Acknowledgements

We thank the New Zealand University Grants Committee for the award of a postgraduate scholarship (to S. B.).

### References

- 1 S. Brooker and V. McKee, *J. Chem. Soc., Dalton Trans.*, 1990, 2397.
- 2 D. Wester and G. J. Palenik, *J. Am. Chem. Soc.*, 1974, **96**, 7565.
- 3 T. J. Giordano, G. J. Palenik, R. C. Palenik, and D. A. Sullivan, *Inorg. Chem.*, 1979, **18**, 2445.
- 4 C. Cairns, S. G. McFall, and S. M. Nelson, *J. Chem. Soc., Dalton Trans.*, 1979, 446.
- 5 M. G. B. Drew, A. H. Othman, and S. M. Nelson, *J. Chem. Soc., Dalton Trans.*, 1976, 1394.
- 6 R. L. Carlin, 'Magnetochemistry', Springer, Berlin, 1986, p. 53.
- 7 W. J. Geary, *Coord. Chem. Rev.*, 1971, **7**, 81.
- 8 J. E. Huheey, 'Inorganic Chemistry: Principles of Structure and Reactivity,' 3rd edn., Harper and Row, New York, 1983, p. 73.
- 9 G. M. Sheldrick, SHELXTL User Manual, Revision 4, Nicolet XRD Corporation, Madison, Wisconsin, 1984.
- 10 G. M. Sheldrick, SHELXS 86, A Program for Crystal Structure Solution, Göttingen University, 1986.
- 11 G. M. Sheldrick, SHELX 76, Program for Crystal Structure Determination, Cambridge University, 1976.

Received 12th February 1990; Paper 0/006621